MATEC Web of Conferences **33**, 06002 (2015)
DOI: 10.1051/matecconf/20153306002

Electrochemical characterization of oxidized nanostructured superelastic Ti-Nb-Zr alloy for medical implants

Yulia Zhukova[1,a], Yury Pustov[1], Vadim Sheremetyev[1], Anton Konopatsky[1], Mikhail Filonov[1] and Vladimir Brailovski[2]

[1]*National University of Science and Technology "MISIS", Leninskiy prosp. 4, Moscow 119049, Russian Federation*
[2]*École de Technologie Supérieure, 1100, Notre-Dame Street West, Montreal (Quebec), Canada H3C 1K3*

Abstract. Metastable Ti-Nb-based shape memory and superelastic alloys are known to be strong candidates for bone implant applications. The issues of the materials' biochemical and biomechanical compatibility and its characterization are reviewed. Thermomechanical treatment is conventionally applied to these alloys in order to obtain supreme functional properties; the processing scheme comprises cold rolling and post-deformation air annealing. The structure and electrochemical characteristics of annealing-induced oxide films were studied by scanning electron microscopy, open circuit potential measurement and voltammetry. It is shown that the samples after the annealing treatment exhibit higher steady-state potential value and lower anodic dissolution current density in simulated biological solution, compared with the samples with mechanically removed oxide films. At the same time, the samples with thermal oxide films exhibited lower rate of passive layer recovery than those subjected to mechanical renewal of the oxidized surface. This fact underlies the recommendation to remove the annealing-induced oxide film from the implants operating under friction conditions.

1 Introduction

One of the major research areas in biomedical materials science is the development of bone replacement materials [1–4]. Metals and alloys are the most widely used materials to manufacture load-bearing implants, including joint prosthesis, dental implants, etc., because of their high strength, ductility and machinability.

Despite of the great progress in this field during the past decades, there is still no perfect material that would fulfil all the strict requirements for such medical devices.

Generally speaking, an implantable material must be biocompatible; moreover, from the "bio-mimicking" standpoint, the structure and properties of a bone-replacing substance should be as close to those of bone as possible [3,4].

The biocompatibility requirements comprise the aspects of biomechanical and biochemical compatibility.

Biochemical compatibility implies the absence of prolonged adverse reactions between host tissues and implanted material. From this standpoint, pure metals can be classified as toxic (Co, Cu, Ni, V), capsule (Fe, Al, Mo, etc.) and vital (Ti, Nb, Ta, Zr, Pt) [5]. In addition to that, the products of corrosion, wear and other medium-assisted degradation processes must be safe for the biological environment.

Biomechanical compatibility is the important property underlying the durability and functional stability of long-term and permanent load-bearing implants. It indicates that the implant's mechanical properties and deformation behavior should be close to those of bone tissue [6]. In particular, the material should have low Young's modulus (ideally adjustable to 1–40 GPa targeting at different types of bone tissue), which would prevent "stress shielding", and support large elastic strains (not less than 0.5 %). Conventional metallic biomaterials like stainless steel, Co–Cr, as well as pure titanium and major part of titanium alloys, fail to meet this requirement.

Possible generally accepted solution for this problem is the development of low modulus titanium alloys comprised of "vital" elements (Nb, Ta, Zr, with Ti as balance) and exhibiting shape memory and superelasticity effect resulting from reversible β to α" martensitic transformation [7–12]; Ti-Nb-based alloys in particular [for example, 13–15].

Conventional metals are spontaneously covered with oxides (TiO_2 in case of titanium) which determine their chemical stability in aggressive environment. When metallic materials are implanted in human body media, initial reactions occur between their surface and the host tissues. Therefore, the surface oxide films play an important role not only against corrosion but also in tissue compatibility.

Metastable Ti-Nb-based alloys exhibit superelastic behavior if they are subjected to a specific sequence of thermomechanical treatment (TMT). The final stage of this TMT comprises air annealing in the 500 to 600 °C temperature range and results in the formation of substantial surface oxide films. The aim of the present study was the preliminary electrochemical

[a] Corresponding author: zhukova@misis.ru (Dr. Yulia Zhukova)

Article available at http://www.matec-conferences.org or http://dx.doi.org/10.1051/matecconf/20153306002

characterization of the oxide layers of Ti-Nb-based alloys; such data for these materials have not yet been reported.

2 Materials and methods

The experimental material was Ti-21.8Nb-6.0Zr (at. %) alloy produced by vacuum-arc melting with consumable electrode and hot-forged, in recrystallized condition, after water-quenching from 900 °C (hereinafter designated as TNZ_0). The samples were further subjected to thermomechanical treatment leading to the formation of nanosubgrain substructure with improved functional properties [8]: cold rolling with a true strain of 0.3, mechanical polishing down to R_a = 0.05 μm of roughness, and 1-hour post-deformation annealing in air at 600 °C with subsequent water quenching. One part of the samples was mechanically polished to remove the oxide layer (samples denoted TNZ_1); another part was studied in as-annealed condition (TNZ_2).

The morphology of oxidized surface was studied by scanning electron microscopy (JEOL JSM-6610LV) using TNZ_2 sample polished cross-section. The samples were mounted in Epofix™ cold-setting embedding resin and mechanically polished. Before the test, a thin conducting layer of graphite was deposited on the surface to form conducting layer.

The immersing medium was Hank's salt solution simulating inorganic components of bone tissue; composition (g l^{-1}): 8 NaCl, 0.4 KCl, 0.12 $Na_2HPO_4 \cdot 12H_2O$, 0.06 KH_2PO_4, 0.2 $MgSO_4 \cdot 7H_2O$, 0.35 $NaHCO_3$, 0.14 $CaCl_2$, H_2O (up to 1 l of the solution); pH = 7.4.

Electrochemical measurements were carried out with electronic potentiostat IPC-Micro by open circuit potential (OCP) and potentiodynamic voltammetry methods (potential scan rate 0.1 mV s^{-1}, starting from steady-state potential value) at (37 ± 1) °C. Saturated silver chloride electrode (hereafter SSCE) was used as a reference electrode, and platinum electrode was used as an auxiliary electrode. Prior to each experiment, all samples were cleaned in distilled water for 10 min using ultrasonic cleaner CT-405.

Due to the fact that the implants performance may be significantly affected by mechanical loads leading to local destruction of passive films formed in biological media, it was considered of practical interest to study the kinetics of passive layer restoration in the case of mechanical renewal. To investigate the self-healing ability of mechanically damaged surfaces in Hank's solution, scratch tests were carried out: the samples were scored with diamond cutter with resulting scratch size of approximately 0.5 × 3 mm.

3 Results and discussion

Fig. 1 shows SEM microphotographs of TNZ_2 sample cross-section containing the annealing-induced oxide film.

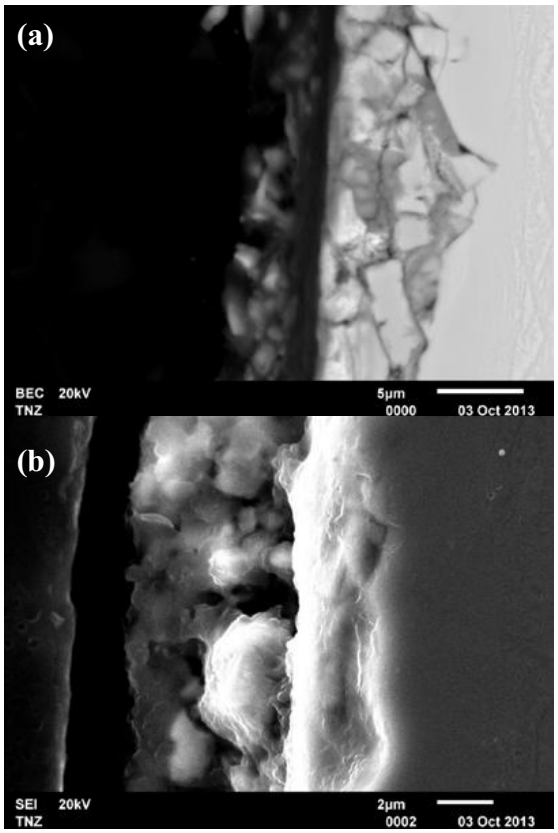

Figure 1. SEM microphotographs of TNZ_2 sample cross-section: backscattered electron image (a), secondary electron image (b).

As seen from Fig. 1 that the annealing-induced oxide film is about 5 μm thick and features through pores about 1 μm in size. This oxide layer may have strong influence on corrosion and electrochemical behavior of the studied alloys, thus electrochemical measurements were carried out on the samples with (TNZ_2) or without (TNZ_1) thermal oxide.

The character of OCP evolution during exposure to simulated solution is an important tool for the investigation of tendency to passivation and protective film formation on the alloy surface.

Fig. 2 shows OCP curves for TNZ samples in Hank's solution.

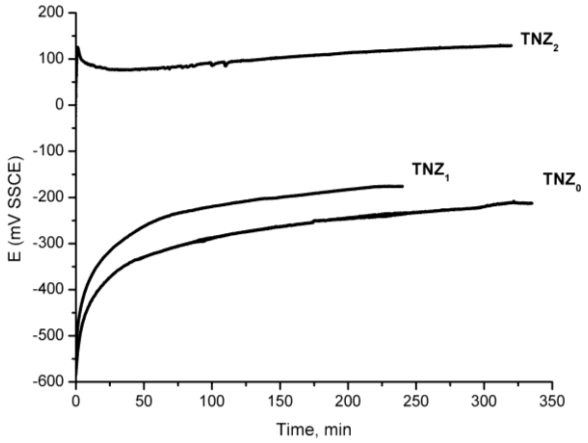

Figure 2. OCP curves for Ti-21.8Nb-6Zr alloy samples in Hank's solution.

It can be seen from Fig. 2 that the OCP values of both the thermomechanically treated and untreated samples shift towards higher values, which is an indication of surface self-passivation.

The steady-state potential value of TNZ_1 sample is markedly higher than that of TNZ_0. This tendency is presumably the result of the nanosubstructure formation in Ti-Nb-Zr alloys during TMT [8]. It is well known that nanostructure formation decreases corrosion resistance when a material corrodes (dissolves) in active mode. However, Ti-based alloys are known to undergo spontaneous self-passivation, and this process is intensified by the surface activation process, which is underlined by the developed network of subgrain boundaries and dislocations; such an increase in corrosion resistance for nanostructured pure titanium has already been reported, for example, in [12].

It is of crucial importance that in case of thermal oxide films, their steady-state OCP is 300 mV higher (TNZ_2) than that of removed films (TNZ_1). The observed OCP shift during the initial period of exposition is presumably related to the clogging of oxide film pores with the resultants of the electrolyte - bare metal reaction.

In order to validate the observed tendency for self-passivation, anodic polarization curves were measured after the establishment of a steady-state OCP (Fig. 3).

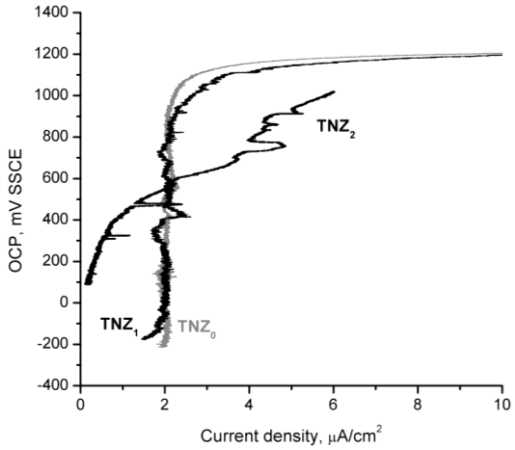

Figure 3. Polarization curves of Ti-21.8Nb-6.0Zr alloy in Hank's solution.

It can be seen from Fig. 3 that the polarization curves lack activation peaks, which is coherent with the OCP measurements, and suggests the tendency to self-passivation. It should be noted that TNZ_2 samples dissolve two times slower during anodic polarization in 200 – 400 mV range than TNZ_1 samples. However, TNZ_1 samples exhibit broader potential range of strong passivity up to the potential of transpassivation or anodic oxygen evolution (~ 1100 mV).

Fig. 4 shows OCP curves of TNZ_1 and TNZ_2 samples in the case of mechanical renewal of the sample surface. It can be seen that TNZ_2 samples after scratching feature significant OCP drop, which indicates the breakdown of passive film with subsequent recovery during ongoing exposition. At the same time, the equal load applied to TNZ_1 samples leads to smaller potential drop with faster film recovery. This fact indicates higher self-healing surface ability in the case of a natural (not thermal) passive oxide layer.

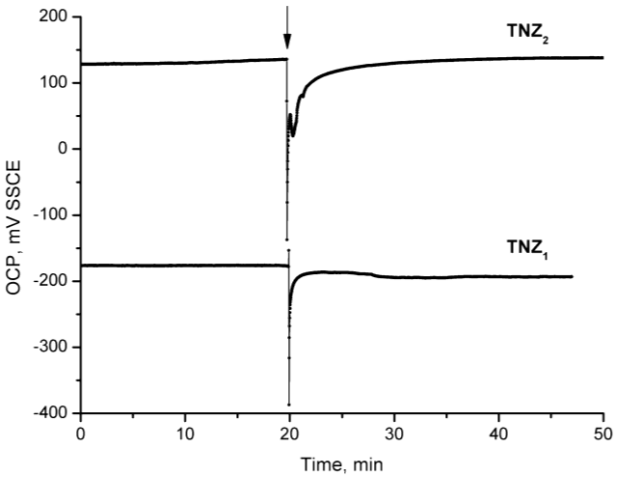

Figure 4. OCP curves for Ti-21.8Nb-6.0Zr alloy after TMT in Hank's solution after mechanical renewal of the sample surface (corresponding time moment indicated with arrow).

In accordance with the methodology for Ti-Nb-based alloys described in [13], the comparative tendency to passivation in simulated solution can be estimated using kinetic regularities of OCP evolution during exposition.

The right part of OCP curves in Fig. 4 (after the surface renewal indicated by arrow) was normalized, i.e. nondimensionalized in 0 – 1 limits. The first part on the processed curves $e\ (t)$ was approximated by the logarithmic equation $e = a + k\ ln\ (t + c)$, where k, a and c are coefficients, with k being the kinetic constant of oxide film growth. The values of the coefficients along with the correlation coefficient for TNZ_1 and TNZ_2 samples are listed in Table 1.

Table 1. Logarithmic approximation results for OCP curves of TNZ_1 and TNZ_2 samples after mechanical renewal of the sample surface.

Sample	k	a	c	R^2
TNZ_1	0.139 ± 0.004	1.023 ± 0.007	0.000 ± 0.000	0.98
TNZ_2	0.125 ± 0.003	0.745 ± 0.003	0.003 ± 0.001	0.91

It can be seen from Table 1 that the kinetic constants of the passive film formation rate k are highly dependent on the presence of thermal oxide on the samples' surface: TNZ_1 samples exhibit 20 – 30 % higher film formation rate than TNZ_2 samples.

4 Conclusion

The influence of thermomechanical treatment (post-deformation annealing in particular) on the electrochemical characteristics of nanostructured superelastic Ti-21.8Nb-6.0Zr (at. %) alloy designed for medical implants is studied.

The general trend is that the TMT annealing-induced micrometer-range oxide films improve the alloys' electrochemical properties in Hank's solution, such as their steady-state electrode potential and anodic dissolution current density. However, it can be recommended to remove the annealing-induced oxide films when implants are to perform in friction conditions, because the passive layer recovery for the samples with the mechanically renewed surface films is faster.

Acknowledgements

The work was carried out with financial support from the Ministry of Education and Science of the Russian Federation (project ID RFMEFI57514X0094).

References

1. J. Park, R. S. Lakes, *Biomaterials – An introduction*, third ed. (Springer-Verlag, New York, 2007)
2. M. Ramalingam, A. Tiwari, S. Ramakrishna, H. Kobayashi (Eds.), *Integrated Biomaterials for Biomedical Technology* (Scrivener Publishing, Beverly, 2012)
3. M. Stevens, Materials Today **11**, 18 (2008)
4. M. Musib, S. Saha, in: T J. Webster (Ed.), *Nanomedicine – Technologies and Applications* (Woodhead Publishing Limited, Oxford, 2012)
5. S.G. Steinemann, in: G.D. Winter, J.L. Leray, K. de Groot (Eds.), *Evaluation of Biomaterials* (Wiley, New York, 1980)
6. M. Niinomi, J. Mech. Behav. Biomed. **1**, 30 (2008)
7. T. Yoneyama, S. Miyazaki, (Eds.), *Shape memory alloys for biomedical applications* (CRC Press – Woodhead Publishing, Boca Raton, 2009)
8. V. Brailovski, S. Prokoshkin, K. Inaekyan, M. Petrzhik, M. Filonov, Yu. Pustov, S. Dubinskiy, Yu. Zhukova, A. Korotitskiy, V. Sheremetyev, in: N. Resnina, V. Rubanik (Eds.) *Shape Memory Alloys: Properties, Technologies, Opportunities* (Trans Tech Publications, Pfaffikon, 2015)
9. H.Y. Kim, Y. Ikehara, J.I. Kim, H. Hosoda and S. Miyazaki, Acta Mater. **54**, 2419 (2006)
10. H.Y. Kim, T. Sasaki, K. Okutsu, J.I. Kim, T. Inamura, H. Hosoda and S. Miyazaki, Acta Mater. **54**, 423 (2006)
11. J.I. Kim, H.Y. Kim, T. Inamura, H. Hosoda and S. Miyazaki, Mater. Sci. Eng. A **403**, 334 (2005)
12. H.Y. Kim, J. Fu, H. Tobe, J.I. Kim and S. Miyazaki, Shape memory and Superelasticity **1**, 107 (2015)
13. J. Fu, A. Yamamoto, H. Y. Kim, H. Hosoda, S. Miyazaki, Acta Biomater. **17**, 56 (2015)
14. V. Brailovski, S. Prokoshkin, M. Gauthier, K. Inaekyan, S. Dubinskiy, M. Petrzhik, M. Filonov, Mater. Sci. Eng. C **31**, 643 (2011)
15. A. Biesiekierski, J. Wang, M. A.-H. Gepreel, C. Wen, Acta Biomater. **8**, 1661 (2012)
16. A. Balyanov, J. Kutnyakova, N.A. Amirkhanova, V.V. Stolyarov, R.Z. Valiev, X.Z. Liao, Y.H. Zhao, Y.B. Jiang, H.F. Xu, T.C. Lowe, Y.T. Zhu, Scripta Mater. **51**, 225 (2004)
17. Yu.S. Zhukova, Yu.A. Pustov, M.R. Filonov, Protection of Metals and Physical Chemistry of Surfaces **48**, 315 (2012)